J. Ocean Univ. China (Oceanic and Coastal Sea Research)
DOI 10.1007/s11802-010-0037-5
ISSN 1672-5182, 2010 9 (2): 1-7
http://www.ouc.edu.cn/xbywb/
E-mail:xbywb@ouc.edu.cn

Solar Radiation Penetrating Through Sea Ice Under Very Low Solar Altitude

ZHAO Jinping*, and LI Tao

College of Physical and Environmental Oceanogrophy, *Ocean University of China*, *Qingdao* 266100, *P. R. China*

(Received February 15, 2010; revised March 3, 2009; accepted March 8, 2009)

Abstract Based on the optical data for transmitted radiation through sea ice in the Arctic during the late autumn and early winter of 2007, the authors studied the arriving solar radiation, reflected radiation and transmitted radiation under very low solar altitude. Through the atmosphere, the light of the arriving solar radiation at short wavelength was weakened, with the spectral distribution of double peaks centered at 490 nm and 683 nm. The magnitude of the peak at 683 nm even exceeded that at 490 nm under the very low solar radiation condition. The reflection was lower than that in summertime because of the thin thicknesses of ice and snow, allowing higher ratio of heat to enter the sea ice and snow. When higher ratio of solar radiation entered sea ice in late autumn, the new ice freezing would be affected. The spectral reflectivity from snow surface was almost a constant, but the reflection without snow decreased at longer wavelengths. In the transmission spectrum, the light of 490 nm was dominant. It indicates that the radiation at longer wavelength was weakened by sea ice. Therefore, under the condition of low solar altitude, the radiation at shorter wavelength was weakened by the atmosphere while the radiation at longer wavelength was weakened by the sea ice. The combined effect of atmosphere and sea ice made the solar radiation under sea ice much weaker. The absorption of sea ice for the longer-wavelength radiation allowed the sea ice to gain more heat to slow down the freezing process.

Key words sea ice; Arctic; optics; solar radiation; solar altitude; transmission

1 Introduction

Sea ice is one of the main climatologic factors in the Arctic, which influences strongly the energy exchange between ocean and atmosphere. In recent years, the ice extent, ice thickness and ice concentration in the Arctic Ocean are declining rapidly and result in an increase of solar energy absorbed by the ocean. The increasing heat flux released by warmer upper ocean positively feeds back to the regional climate (Curry *et al.*, 1995; Holland *et al.*, 2006) and influences eventually the global climate significantly (Parkinson *et al.*, 1999; Lindsay and Zhang, 2005).

Sea ice is a result of phase change of seawater in cold season. The complex structure of sea ice influences the absorption of solar energy (Hobbs, 1974; Perovich *et al.*, 1998). The solar energy penetrating through sea ice and entering seawater (hereafter referred to as 'transmission') is the main heat source of high-latitude ocean, which directly impacts local ice melting and freezing (Perovich, 1996; Zhao *et al.*, 2009). The amount of photons entered seawater in summertime is a key factor for biomass productivity under sea ice and partly determines the state of marine ecosystem (Grenfell *et al.*, 2006). The solar radiation arriving at the surface of sea ice is easy to measure. The transmission, however, is much more difficult to observe, but it is necessary to make such observation for estimating the heat absorbed by sea ice and seawater.

Because the transmission of solar radiation through sea ice is closely related to ice thickness, an optical instrument must be put under sea ice to measure the transmissivity (Grenfell, 1979). Early observations of transmission were operated by divers who brought an instrument to make direct measurement, which was time consuming, for a big hole needed to be dug through the ice for each measurement (Maykut and Grenfell, 1975). The situation was much improved after the self-recording spectrophotometer was developed in early 1970s. The instrument itself can be put under sea ice with a small hole, which makes it possible to measure the transmission radiation in a larger area (Roulet *et al.*, 1974). The transmission measurement has become a unique means to observe reliably the solar radiation absorbed by sea ice and seawater. The optical observation under sea ice is more significant for the first-year ice, through which more solar energy is absorbed and transmitted. The transmission data are usually used to obtain solar radiation heating for sea ice (Hamre *et al.*, 2004), influence of light on photosynthesis in marine ecosystem (Trodahl and Bucklay, 1989; Donald and Perovich, 1995), and influence of biomass on light

* Corresponding author. Tel: 0086-532-66781820
E-mail: jpzhao@ouc.edu.cn

absorption in the upper ocean (Grenfell *et al.*, 2006). However, the observation of transmission is still rare as the field work has to be conducted on ice, which requires special logistics, such as small boat, helicopter, and heavy equipments, among others. Ship time and ice condition are other factors to restrict transmission measurement.

Most of the limited transmission data were obtained during ice melting season in summer, and few were reported in spring and autumn. In autumn, the solar altitude is very low, slightly above the horizon, and the arriving solar energy is much weaker than that in summer. However, autumn is the ice freezing season; any unweighted change of solar radiation will in fact influence the freezing speed and growth of ice thickness. During the ice freezing period, the heat exchange through the thin ice is more remarkable and sensible than that through thick ice, the influence on Arctic atmospheric process being not neglectable. The observation of transmission under very low solar altitude can measure spectral solar energy penetrating through sea ice, and therefore benefits studying the air-sea interaction during the ice freezing season.

In this paper, the spectral feature of incident solar radiation, radiation through sea ice and the rates for reflection and transmission are studied based on the in situ observation data under very low solar altitude in the Arctic in late autumn. The influence of solar radiation on ice freezing process is also discussed.

2 Field Measurement

A year-round cruise organized by the Circumpolar Flaw Leads (CFL) Study project of Canada was implemented in the Arctic, including the regions of the Amundsen Bay and the Beaufort Sea, and operated by Canadian Coast Guard icebreaker, the *Amundsen*. We were involved in the Leg-4 of the cruise from November 8 to December 20, 2007. At the early stage of the leg, the solar altitude was very low and the daytime was very short, which provided us a precious opportunity to observe the solar radiation with very low solar altitude. During the cruise, sea ice covered the sea surface, the ice thickness grew quickly, and the weather was cold and stormy.

In many of the observations made during the Leg-4, only few measurements were conducted during daytime. The first observation was on November 15, and the polar night started on November 22, with only eight days to measure solar radiation. Since the time window of noon was very short, sometimes we missed the observation window. Only the data at four stations were available to illustrate the property of solar radiation with solar altitude lower than 5°. All the stations were located in the Amundsen Gulf as shown in Fig.1. Information of the stations is listed in Table 1.

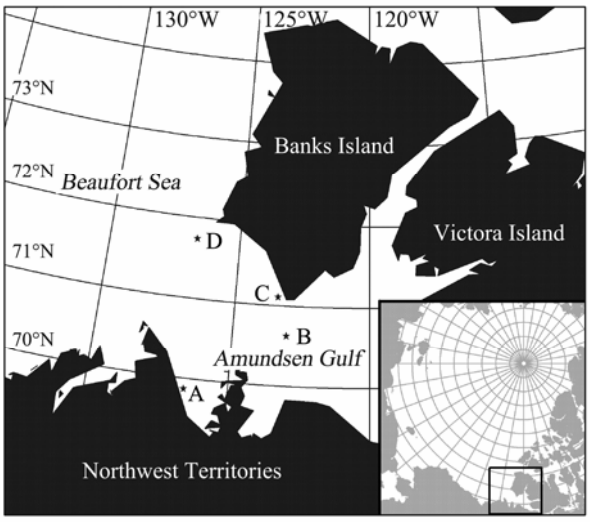

Fig.1 Sketch of the Amundsen Bay in the Arctic and the stations. The location of the Amundsen Bay is given in the lower right corner.

Table 1 Information of stations for location, solar radiation, ice and snow

Station	Station ame	Date	Solar time	Location	Area	Radiation (W m^{-2})	Ice thickness (cm)	Snow thickness (cm)	Cloud
A	1117	11-16	12:42	126°32.541′W 69°52.301′N	Nearshore	8.17	34	1	No
B	405	11-19	10:03	123°02.263′W 70°37.767′N	Deep sea	3.41	42	1	No
C	1100	11-20	13:33	123°24.693′W 71°06.473′N	Nearshore	0.87	110	3	Cloudy
D	437	11-22	11:09	126°39.297′W 71°44.232′N	Deep sea	1.72	56	1	Cloudy

The four measurements were obviously not enough to describe the transmitted radiation through sea ice under very low solar altitude in a large area. However, the data were so precious since it allowed us to understand the transmitted radiation under such a unique condition of late autumn and early winter. The instrument we used was the Profiling Reflectance and Radiometer made by the Biosphere Inc. of the U.S., which included two parts. The PRR-800 was an underwater system for measuring downwelling and upwelling radiations in seawater, and the PRR-810 was a unit used in the air to measure the downwelling radiation arriving at the surface and the reflection. Eighteen wave-lengths were equipped in the PRR instrument; they were 313, 380, 412, 443, 465, 490, 510, 532, 555, 565, 589, 625, 665, 683, 710, 765, 780 and 875 nm, covering the spectral range from ultraviolet to infrared. Most spectral measurements were perfect with the exception of 313 nm, which was strongly impacted by

the substance inside the sea ice. An undisturbed flat ice with a large area was chosen for measurement and a hole of 20 cm in diameter was drilled by a Jeffy auger. The instrument was put into seawater through the hole with a rotatable link gear. By turning the gear to 90°, the instrument was attached under sea ice vertically with a tilt less than 2°. Then, the hole was blocked by opaque material to avoid any disturbance from surface light. A computer was used to control the measurement and collect data in real time. The measuring geometry is shown in Fig.2.

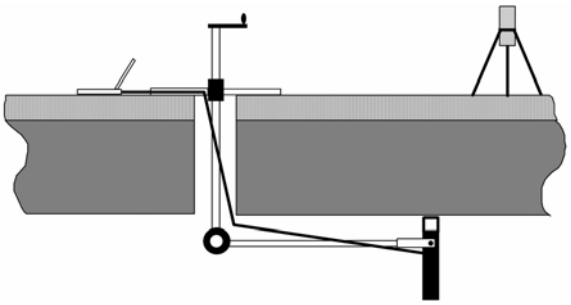

Fig.2 Sketch of deployment for the PRR optical system.

The instrument PRR-810 kept its face upward vertically to measure the downwelling radiation for one minute. Then, the instrument was turned to face downward to measure the upwelling reflecting radiation with the instrument set 1-m above the ice surface. During the surface measurement, the underwater unit PRR-800 was making simultaneous record to provide the reference data in calculating the reflection.

A typical measurement at Station C with ice thickness of 110 cm and snow depth of 3 cm is shown in Fig.3. The underwater instrument was recording continuously during the whole measurement period (thin solid line). The surface instrument was kept recording as well, but its cover was only opened during the measurement as indicated by the thick solid line. The radiation intensity decreased quickly during the one-minute measurement. The noise appearing on the line was caused by the turnover of the instrument. The four stairs from left to right are reflections by snow, incident with snow, incident without snow and reflection without snow, respectively. The radiation intensity decreased quickly during the 6.4-minute measurement when the solar altitude was very low, about 2° or so.

Hanesiak *et al*. (2001) measured the radiation by a remote cosine receptor (RCR) in a similar way. They measured the downwelling radiation first and then made the instrument turnover to measure the spectral reflection. A foreoptics was added in front of the instrument to reduce the field of view (FOV) from 180° to 26° in order to shorten the reflecting range, but it was impossible to use RCR under very low solar altitude. Bélanger *et al*. (2007) considered the rapid attenuation of the sunlight in measuring the reflection. He used two spectroradiometers made by FieldSpec, Analytical Spectral Devices Inc.: one was to measure downwelling radiation and upwelling radiation, and the other, to measure downwelling radiation E_d^{ref} as a reference. To ensure the accuracy of reflection in previous studies, one instrument was used when the solar radiation varied slowly and two instruments were needed when the solar radiation varied rapidly.

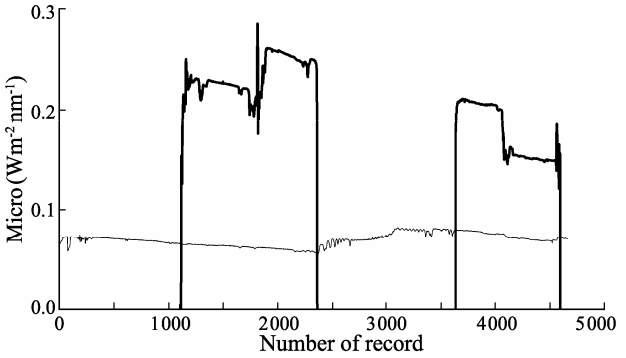

Fig.3 Measured results at Station C for incidence, reflection and transmission at 465 nm. The thick line gives incident and reflected radiations by surface instrument PRR-810, and the thin line shows transmitted radiation by under ice PRR-800. Twelve values were recorded per second.

For a rapid variation of solar radiation, we ensured the measuring accuracy by simultaneous recording of surface and underwater instruments. The only assumption was that the reflectivity and transmittivity of light through sea ice keep unchanged during the 5–6 minute measurement, which is reasonable as the ice physics properties change little in such a short time. For varying incident and transmitted radiation, the spectral transmittivity $\gamma(\lambda)$ and reflectivity R needs to be averaged within the measuring time span, τ, namely,

$$\gamma(\lambda)=\frac{1}{\tau}\int_0^{\tau}\frac{E_{dw}(\lambda)}{E_d(\lambda)}\mathrm{d}t\,, \tag{1}$$

$$R(\lambda)=\frac{1}{\tau}\int_0^{\tau}\frac{E_r(\lambda)}{E_d(\lambda)}\mathrm{d}t\,, \tag{2}$$

where $E_d(\lambda)$、$E_r(\lambda)$ and $E_{dw}(\lambda)$ are incident radiation, reflected radiation and transmitted radiation under sea ice, respectively. After obtaining the spectral reflectivity, the albedo can be calculated by (Wadhams, 2000)

$$\alpha=\frac{\int R(\lambda)E_d(\lambda)\mathrm{d}\lambda}{\int E_d(\lambda)\mathrm{d}\lambda}\,. \tag{3}$$

The measurement was divided into two stages. First, observation was made with the snow lying on the ice, and then the snow was cleared in a large area to observe the bare ice. The radiation at low solar altitude was not only weak, but also rapidly changed with time, so the measurement must be done very quickly to avoid the error caused by changing radiation.

3 Incident and Reflecting Radiation

3.1 Local Solar Time

Owing to the very short daytime just before the polar

night, the radiation characteristics are related to local solar time. It is necessary to calculate the local solar time to determine the time difference from noon. The universal time (UTC) was used to record the observation time, which benefited calculation of solar time T_{solar} by the following equation (Watt Engineering Ltd., 1978)

$$T_{solar}=UTC+E_t/60+L/15, \quad (4)$$

where L is the exact longitude of the measuring location, and E_t is the time equation, a time difference caused by the Earth rotation surrounding the Sun and the angular momentum conservation. In November, E_t can be calculated by (Watt Engineering Ltd., 1978)

$$E_t=16.4\sin(\pi\frac{n-247}{113}). \quad (5)$$

As listed in Table 1, the local solar times of the four stations were all within two hours from noon.

3.2 Incident Solar Radiation

The intensity of the arriving solar radiation was weak because of cloudiness and lower solar altitude. All of the solar radiation records were lower than 10 W m^{-2}, which was insufficient to offset the heat loss from the ice surface, and the ocean was losing heat as a result.

The spectral distributions of incident and reflecting solar radiations at the snow surface are plotted in Fig.4. There were two peaks of incident radiation occurring at 490 nm and 683–780 nm (referred to as 'peak of 683 nm') (Maykut and Grenfell, 1975), respectively. The exact wavelength of the peaks depends on the spectral resolution of the instrument. The reflection was weaker but similar to the incident radiation in its spectral distribution. There was obvious difference of solar radiation at different stations. At Stations A and D, the peak of 490 nm was higher than that of 683 nm, while the two peaks of radiation were nearly the same at Stations B and C, showing the weakening of the peak of 490 nm there.

By calculating the local solar time, the time deviations at the four stations from noon were 42, 117, 87, 51 min, respectively. It is indicated that the difference of the two peaks was larger when the solar altitude was relatively high in the cases of Stations A and D. The difference of the two peaks was reduced when the time deviation from noon was larger and the solar altitude became lower. The two-peak structure was also observed in the Bohai Sea, as indicated by Yue *et al.* (2000) and Qu *et al.* (2009), but the peak of 683 nm nearly vanished, as the latitude of the Bohai Sea is around 40°N and the solar altitude is higher than 70° around noon. These results support the notion that the higher the solar altitude is, the weaker the peak of 683 nm becomes. In other words, the radiation of 490 nm is strongly weakened under very low solar altitude. Sinice 490 nm is the strongest radiation band of the Sun and there is no main absorption in the atmosphere around this wavelength, the decrease at this wavelength must be caused by the scattering of light in the atmosphere. Stronger scattering under very low solar altitude decreases the solar energy arriving at the earth surface.

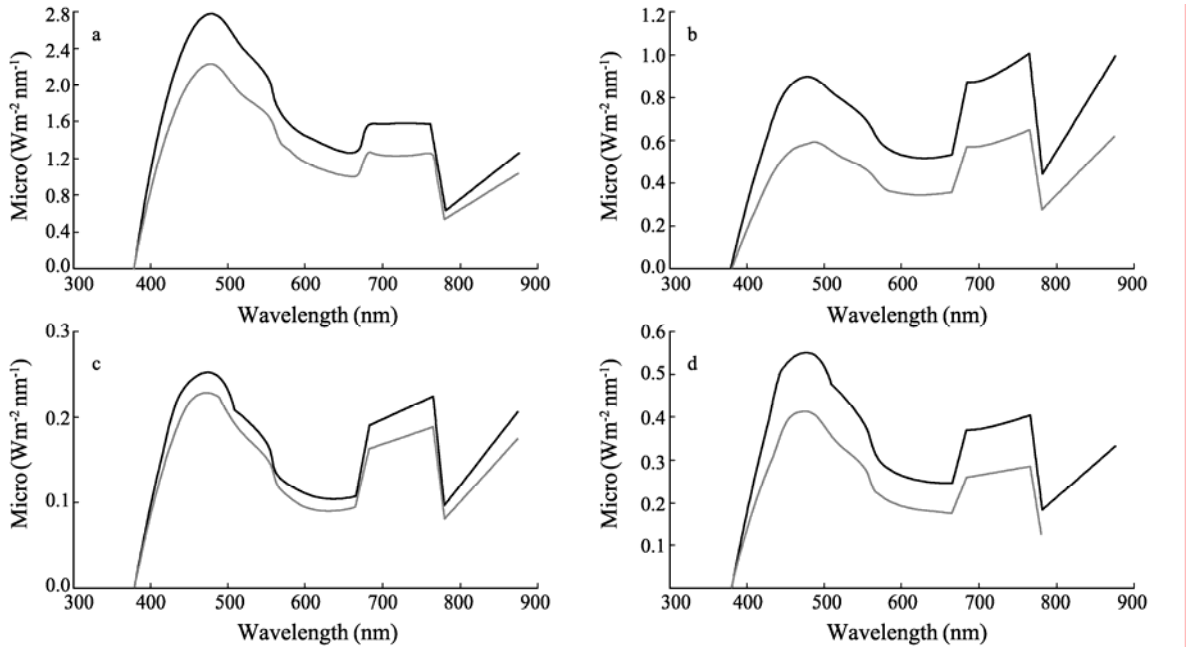

Fig.4 Spectral irradiance (thick line) and reflection (thin line) of solar radiation at each station with snow.

3.3 Reflection from the Snow and Ice

Since the transmission of light was closely related to the reflection of the surface, the spectral reflection was measured at the same location with the downwelling radiation.

The spectral reflectivity was different at each location as shown in Fig.5. The snow depths at the four stations were all very thin, but their effect on reflection was obvious as the reflectivity was above 0.6 at all stations. It looks like the reflectivity from snow surface was not much correlated with ice thickness, because the reflectiv-

ity with minimum ice thickness at Station A and that with maximum ice thickness at Station C were nearly the same. The reflectivity without snow was reduced differently with spectrum. Main reduction of reflection from ice surface appeared at the long-wave part of the spectrum, suggesting more long-wave radiation was absorbed by sea ice. The unchanged reflections with and without snow appeared at different wavelengths, 400–500 nm at Stations B and C, and 600 nm at Station D. At Station B, the reflectivity with and without snow was similar, because the snow was embedded into the rough ice surface and formed a high-reflection layer.

Albedo calculated by Eq. (5) was all above 0.6 as shown in Fig.6, regardless of having snow or not. The albedo was much lower than that measured in summertime (Zhao *et al*., 2009) because of the thin ice and snow. It means that, under very low solar altitude, a higher ratio of the solar radiation entered the sea ice and ocean to influence ice freezing, though the intensity of solar radiation then was weak.

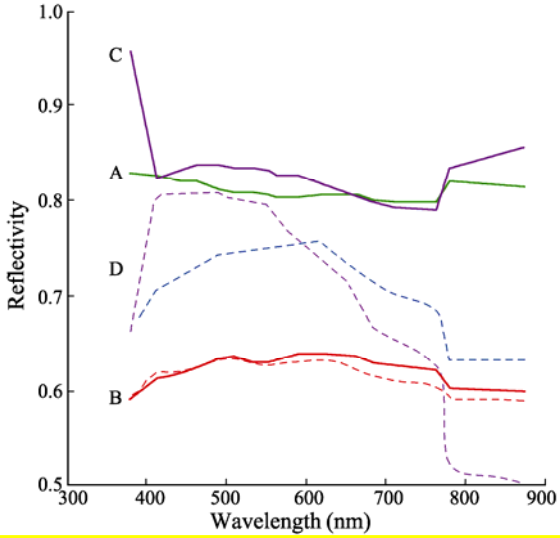

Fig.5 Spectral reflectivity at each station with snow (solid lines) and without snow (dashed lines).

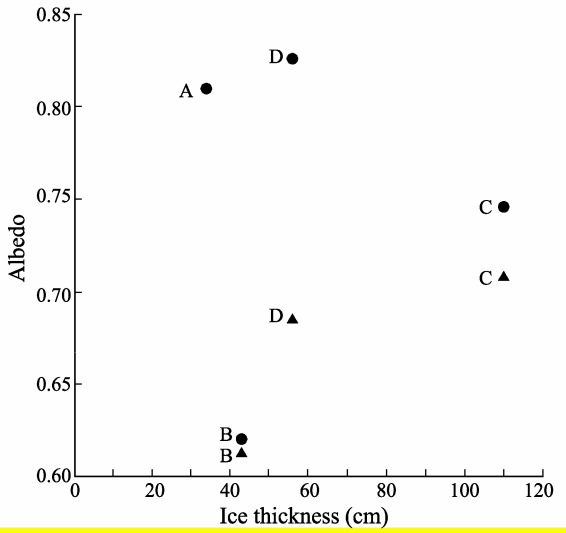

Fig.6 Relationship between albedo and ice thickness for snow-covered (dot) and snow-free (triangle) situations at various stations.

4 Characteristics of Transmitted Radiation

Transmission is the solar radiation penetrating through sea ice and arriving at the surface of seawater underneath. Transmission radiation is not only related to the solar radiation arriving at the ice surface but also influenced by the crystal structure, brine, bubble, and other substances inside sea ice (Perovich, 1996).

4.1 Spectral Distribution of Transmitted Radiation Flux

Based on the geometric optics, most of the solar energy arriving at ice surface will be reflected or scattered back to space when the incident angle is close to 90°. The measurement result shows that, however, a certain part of the solar energy reached seawater by light refraction in sea ice.

As shown in Fig.7, the maximum transmission radiation flux appeared at 490 nm, being well consistent with the peak of solar radiation except at Station D where it was at 465 nm. The transmission at Station C was very weak as the ice was thick than 1 m. Abrupt change occurred at all stations at 780 nm and then the transmission decreased to zero. It means that sea ice strongly absorbed the red and infrared light, and only the light with wavelength of 380–780 nm could penetrate sea ice and arrived at the seawater underneath.

The solar radiation arriving at snow surface contained a peak at 683 nm as indicated in Section 3.1 (Fig.4); however, the peak was greatly weakened or even diminished by sea ice in the transmitted radiation at all stations (Fig.7). The intense absorption of the water molecules composing of sea ice is speculated to weaken the light of 683 nm, as the water in solid and liquid states are similar in absorbing long-wave radiation (Perovich, 1996).

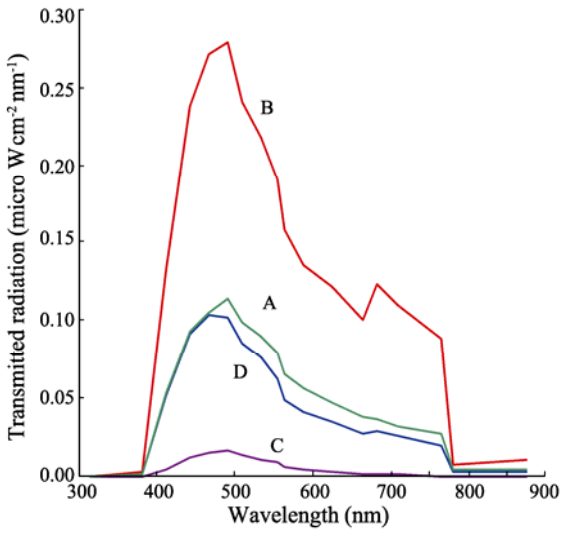

Fig.7 Spectral transmittivity of solar radiation under snow-covered ice.

4.2 Spectral Distribution of Transmittivity

The spectral distribution of the transmittivity with snow (solid lines) and without snow (dashed lines) is

shown in Fig.8 (no observation for the case without snow at Station A). It shows clearly that the transmission was influenced by ice thickness. The transmittivity of sunlight through thin sea ice without snow was high. With ice thickness of 35 cm at Station B, 35% of the sunlight was transmitted. At Station C with ice thickness of 110 cm, however, the maximum transmittivity was only 2% or so. The highest transmission appeared at 490 nm, showing its best penetrating capacity through sea ice.

The characteristic of bulk transmittivity vs. ice thickness is shown in Fig.9. As Station A was located in a semi-enclosed bay, there was rich particulate materials in the sea ice and the transmittivity was very low. Besides, at Stations B, C and D, the transmittivity was inversely proportional to the thickness of ice both with and without snow. The light transmittivity through sea ice in deep water was higher as in the cases of Stations B and D. Due to the limited data, it is not yet possible to simulate the variation of transmittivity with ice thickness by a regressive function.

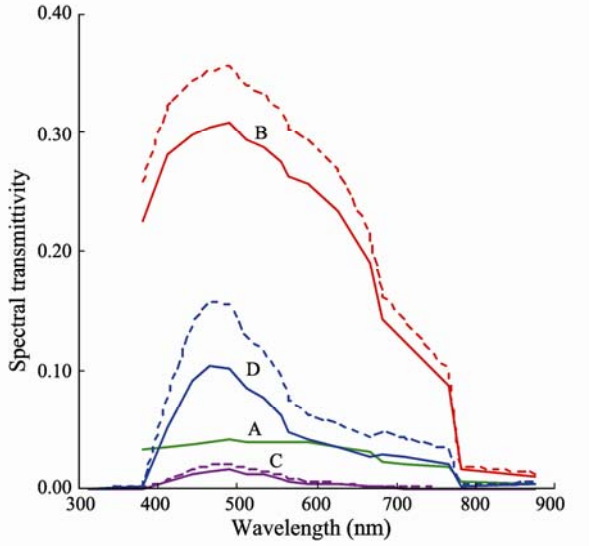

Fig.8 Spectral transmittivity with snow (solid lines) and without snow (dashed lines).

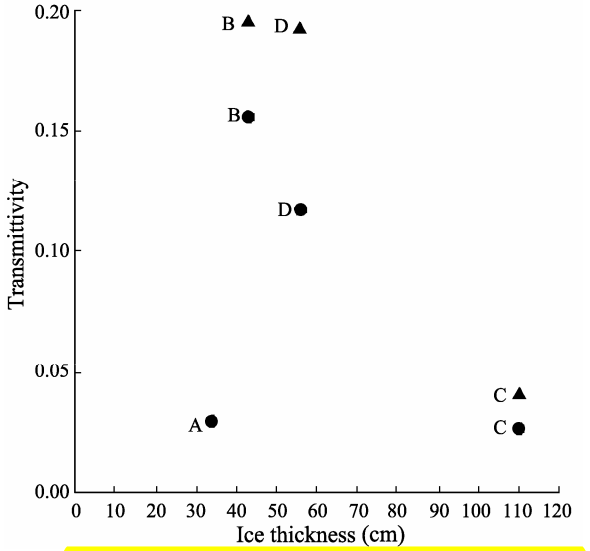

Fig.9 Relationship between transmittivity and ice thickness for the snow-covered (dot) and snow-free (triangle) situations.

5 Results and Discussion

Based on the field data of optical transmission through sea ice obtained by the authors in the Amundsen Gulf in 2007 winter, the incident spectral solar radiation, reflection and transmission through sea ice under very low solar altitude were studied. The influence of solar radiation on freezing of the new ice was analyzed. The results of this paper are significant for the studies on ice freezing in late autumn and early winter when the solar altitude is low over a long time.

Through the atmosphere, the arriving solar radiation with short wavelength was weakened for the very low solar radiation, and that with longer wavelength remained. The spectral distribution of the arriving solar radiation appeared with double peaks centered at 490 nm and 683 nm. The double peaks appeared more evident when the solar altitude was lower. The peak of 683 nm even exceeded that of 490 nm under the very low solar radiation condition.

Although the solar altitude was low, the reflectivity of light was lower than that observed in summertime, as the sea ice was newly frozen and the snow cover was thin. It meant a higher ratio of solar radiation entering the sea ice in late autumn though the solar radiation was then very weak, which would influence the freezing. The spectral reflectivity from snow surface was almost constant with little difference with respect to wavelength, whereas the reflection without snow decreased with increasing wavelength because of stronger absorption ability of sea ice for the light with longer wavelength.

In the transmission spectrum, the light of 490 nm again dominated. The 683-nm peak of the solar radiation arriving at the surface nearly vanished from the transmission spectrum. It indicates that the light with longer wavelength was weakened by sea ice; the thicker the sea ice was, the weaker the 683-nm peak was. The reason is that the light absorption of sea ice is similar to that of seawater, namely the former absorbs strongly the longer wavelength radiation.

In summary, under low solar radiation the light with shorter wavelength is weakened in the atmosphere, whereas the light with longer wavelength is weakened in the sea ice. The combined effects of atmosphere and sea ice make the solar radiation under the sea ice much weaker. The absorption of sea ice at the longer wavelength allows the sea ice to gain more heat to slow down the freezing process.

Acknowledgements

This study was supported by the key project of the National Nature Science Foundation of China 'Study on the structure of Arctic Circumpolar Boundary Current and its impact on climate change' (Grant No. 40631006), and by the Chinese International Polar Year Project. The field observation was supported by Professor David Barber at the University of Manitoba of Canada. We greatly appre-

ciate the effort and help by the captain and crew of the *Amundsen* during the cruise.

References

Bélanger, S., Ehn, J., and Babin, M., 2007. Impact of sea ice on the retrieval of water-leaving reflectance, chlorophyll a concentration and inherent optical properties from satellite ocean color data. *Remote Sens. Environ.*, **111**: 51-68.

Curry, J. A., Schramm, J. L., and Ebert, E. E., 1995. Sea ice-albedo climate feedback mechanism. *J. Clim.*, **8**: 240-247.

Donald, K., and Perovich, D. K., 1995. Observations of ultraviolet light reflection and transmission by first-year sea ice. *Geophys. Res. Lett.*, **22** (11): 1349-1352.

Grenfell, T. C., 1979. The effect of ice thickness on the exchange of solar radiation over the polar oceans. *J. Glaciol.*, **22**: 305-320.

Grenfell, T. C., Light, B., and Perovich, D. K., 2006. Spectral transmission and implications for the partition in shortwave radiation in arctic sea ice. *Ann. Glaciol.*, **44**: 1-6.

Hamre, B., Winther, J. G., Gerland, S., Stamnes, J. J., and Stamnes, K., 2004. Modeled and measured optical transmittance of snow-covered first-year sea ice in Kongsfjorden, Svalbard. *J. Geophys. Res.*, **109**, C10006, doi:10.1029/2003JC001926.

Hanesiak, J. M., Barber, D. G., De Abreu, R. A., and Yackel, J. J., 2001. Local and regional albedo observations of Arctic first-year sea ice during melt ponding. *J. Geophys. Res.*, **106** (C1): 1005-1016.

Hobbs, P. V., 1974. *Ice Physics*. Oxiford University Press, London, 837pp.

Holland, M. M., Bitz, C. M., Hunke, E. C., Lipscomb, W. H., and Schramm, J. L., 2006. Influence of the sea ice thickness distribution on polar climate in CCSM3. *J. Clim.*, **19** (11): 2398-2414.

Lindsay, R. W., and Zhang, J., 2005. The thinning of Arctic sea ice, 1988–2003: have we passed a tipping point? *J. Clim.*, **18** (22): 4879-4894.

Maykut, G. A., and Grenfell, T. C., 1975. The spectral distribution of light beneath first-year sea ice in the Arctic Ocean. *Limnol. Oceanogr.*, **20** (4): 554-563.

Parkinson, C. L., Cavalieri, D. J., Gloersen, P., Zwally, H. J., and Comiso, J. C., 1999. Arctic sea ice extents, areas and trends, 1978-1996. *J. Geophys. Res.*, **104** (C9): 20 837-20 856.

Perovich, D. K., 1996. *The Optical Properties of Sea Ice*. Monograph 96-1, US Army Corps of Engineers, Cold Regions Research & Engineering Laboratory, 25pp.

Perovich, D. K., Roesler, C. S., and Pegau, W. S., 1998. Variability in Arctic sea ice optical properties. *J. Geophys. Res.*, **103** (C1): 1193-1208.

Qu, P., Zhao, J. P., Li, S. J., Cao, W. X., and Xu, D. Z., 2009. Spectral features of solar radiation in sea ice of Bohai Sea. *Acta Oceanol. Sin.*, **31** (1): 37-43 (in Chinese with English abstract).

Roulet, R. R., Maykut, G. A., and Grenfell, T. C., 1974. Spectrophotometers for the measurement of light in polar ice and snow. *Appl. Opt.*, **13**: 1652-1659.

Trodahl, H. J., and Bucklay, R. G., 1989. Ultraviolet levels under sea ice during the Antarctic spring. *Science*, **245** (4914): 194-195.

Wadhams, P., 2000. *Ice in the Ocean*. Gordon and Breach Science Publishers, London, 351pp.

Watt Engineering Ltd., 1978. On the Nature and Distribution of Solar Radiation, US Government Printing Office Stock 1978, No. 016-000-00044-5.

Yue, Q. J., Ji, S. Y., Miao, W. D., and Wu, S. L., 2000. Solar radiation on sea ice in Liaodong Bay. *Oceanol. Limnol. Sin.*, **31** (5): 562-567 (in Chinese with English abstract).

Zhao, J. P., Li, T., Zhang, S. G., and Jiao, Y. T., 2009. The shortwave solar radiation energy absorbed by packed sea ice in the central Arctic. *Adv. Geosci.*, **24** (1): 34-42 (in Chinese with English abstract).

(Edited by Xie Jun)